



Dual versus single energy cardiac CT to measure extra cellular volume in cardiac amyloidosis: Correlations with cardiac MRI

Anahita Tavoosi^a, Juliana Brenande de Oliveira Brito^b, Huda El Mais^a, Toby D. Small^a, Andrew M. Crean^a, Benjamin J.W. Chow^a, Gary R. Small^{a,*}

^a Division of Cardiology, Department of Medicine, University of Ottawa, Ottawa, Ontario, Canada

^b Beneficiencia Portuguesa de Sao Paulo, 769 Maestro Cardim St, Bela Vista, Sao Paulo 01323-001, Brazil

ARTICLE INFO

Keyword:

Extracellular volume
Dual energy cardiac CT
Cardiac amyloid

ABSTRACT

Rationale and objectives: Determine in cardiac amyloid (CA) patients, whether cardiac CT derived extracellular volume (ECV) correlates with that obtained by MRI. Perform this correlation with single (SECT) versus dual energy (DECT) CT and evaluate whether a single sample volume ECV-measure was as reliable as a global (16 segment) assessment.

Materials and methods: CA patients who had undergone a clinical cardiac MRI (CMR) were recruited prospectively. SECT and DECT cardiac scans were performed. Three ECG-triggered prospective SECT scans were acquired: non-contrast, arterial-phase contrast and 5-minute delayed images. A DECT scan was performed at 7 min. Post processing was used to determine ECV. Analyses of SECT or DECT global ECV versus CMR were performed using the Pearson correlation coefficient, Bland Altman analysis and Intraclass correlation coefficient (ICC). Similar analyses were performed to examine the performance of single-segment sampling by SECT or DECT versus CMR.

Results: 25 patients were recruited, mean age was 80.0 ± 7.1 years, 80 % were male, 21 patients had transthyretin-CA, 4 had light chain-CA. Correlations were close with both SECT or DECT global ECV versus CMR ($r = 0.79$ and 0.88 respectively, $p < 0.001$ for both). Reliability of both SECT and DECT to assess global ECV in comparison to CMR was good: ICC for SECT was 0.88 (95 % CI 0.73 – 0.95) and 0.93 (95 % CI 0.82 – 0.97) for DECT. For single volume sampling techniques: correlations were close with both SECT or DECT versus CMR ($r = 0.60$ and 0.72 respectively, $p < 0.01$ for both) There was no difference in ICC for SECT (0.74 , 95 % CI 0.41 – 0.88) versus DECT (0.84 , 95 % CI 0.63 – 0.93). Wider confidence intervals were noted for ICC with single versus global CT derived ECV assessment. Mean effective radiation dose was for SECT was 5.49 ± 8.04 mSv and 6.90 ± 3.01 mSv for DECT dual energy CT ($p = 0.75$).

Conclusions: Global ECV values derived by both DECT or SECT correlated with those obtained by CMR and demonstrated good reliability by ICC in a population of CA patients. DECT and SECT single sampling derived ECV values also demonstrated close correlation and good reliability but the ICCs for single sampling had wider confidence intervals than global ECV assessment.

1. Introduction

Myocardial extracellular volume (ECV) quantifies non-cellular material within the myocardium [1]. It varies modestly in health and increases considerably in disease [2]. ECV increases are attributed to localized fibrous scar material, they can also be the result of edema or a more diffuse protein infiltration. Diffuse myocardial protein infiltration

characterizes cardiac amyloidosis (CA) [3]. Distinctive, very large increases in ECV are therefore associated with CA and can be of diagnostic utility [4].

ECV has been quantified from histology and correlated with non-invasive measures [5]. The commonest technique for non-invasive ECV assessment is cardiac magnetic resonance (CMR) scanning [1]. CMR uses the paramagnetic effect of gadolinium on adjacent water molecules

Abbreviations: SECT, Single energy- CT; DECT, Dual energy- CT; ECV, Extracellular volume; CA, Cardiac amyloidosis.

* Corresponding author.

E-mail address: gsmall@ottawaheart.ca (G.R. Small).

<https://doi.org/10.1016/j.ijcha.2022.101166>

Received 8 December 2022; Received in revised form 15 December 2022; Accepted 17 December 2022

2352-9067/© 2022 The Author(s). Published by Elsevier B.V. This is an open access article under the CC BY-NC-ND license (<http://creativecommons.org/licenses/by-nc-nd/4.0/>).

to determine ECV [6]. Iodine contrast media used in cardiac CT is, like gadolinium, water soluble and readily diffuses into the myocardial extracellular space to enable ECV assessment by CT. Measurement of ECV with cardiac CT methods have demonstrated accurate correlation with histology and CMR [3,6]. CT is more widely available than CMR. Since the diagnosis of CA is difficult and typically delayed 1–2 years the increased availability of CT derived ECV could reduce the delays to diagnosis in CA [7].

The measurement of ECV with CT has been performed using different protocols. Some have utilized a conventional single tube potential/single energy approach while others have employed advanced CT-perfusion techniques [6,8]. Dual tube potential or dual energy protocols have also been used [9,10]. While most of the CT techniques have been validated against CMR. Few studies have compared single energy CT with dual energy protocols [11].

Therefore, in this study we sought to compare two CT protocols to assess ECV in CA patients: dual energy versus single energy. We also wished to assess the utility of a single myocardial sample volume versus a global myocardial assessment to establish an optimal clinical approach.

2. Methods

From June 2020 until August 2022 patients with cardiac amyloid were recruited. The study was awarded ethical approval by the Ottawa Health Science Network Research Ethics Board. All patients provided informed written consent. The diagnosis of CA was confirmed clinically via ^{99m}Tc-pyrophosphate scanning, characteristic CMR appearances and positive bone marrow findings, or endomyocardial biopsy [14]. Exclusion criteria included advanced renal dysfunction (eGFR < 30 ml/min/1.73 m²), the presence of an implantable cardiac electronic device, iodine or gadolinium contrast dye allergy, claustrophobia, or clinical contra-indication to cardiac CT or CMR.

2.1. Cardiac magnetic resonance imaging

CMR acquisition was performed as per clinical routine on a 1.5 T unit (Siemens Healthineers, Erlangen, Germany) according to standardized protocols [15]. The protocol included a) short axis steady state free precession (SSFP) cine imaging in short axis (slice thickness 8 mm, gap 2 mm) from base to apex; b) inline motion-corrected native T1 and T2 maps in the short axis at basal, mid and apical levels as well as in the 3 and 4 chamber positions; c) dynamic resting perfusion; d) post contrast axial T1-VIBE images; e) post contrast SSFP single slice 2, 3 and 4 chamber cine imaging; f) single shot and segmented inversion recovery gradient echo late gadolinium enhancement (LGE) images 10 min-15 min after single-dose (0.1 mmol/kg) of macrocyclic Gadobutrol (Gadavist, Bayer Healthcare Pharmaceuticals Inc, Leverkusen, Germany); and g) post contrast T1 maps to match the native T1 slices.

2.2. CMR-ECV analysis

ECV analysis was performed using dedicated cvi42 software (Circle Cardiovascular Imaging, Calgary Canada). LV myocardial regions of interest (ROIs) were drawn on basal, mid and distal SSFP short axis T1 slices pre and post contrast. T1 LV blood pool value was measured with a manual ROI (≥ 100 mm²), excluding the papillary muscles. A 16 segment ECV polar map was generated as per clinical practice using the equation [6]:

$$(\text{ECV (CMR)}) = (1 - \text{hematocrit}) * ((\Delta 1 / \text{T1 myocardium}) / (\Delta 1 / \text{T1 blood})) * 100.$$

2.3. Cardiac CT imaging

CT scans were performed using the Siemens Somatom definition flash 128 dual source scanner (Siemens Healthineers Erlangen,

Germany). Briefly, four CT scans were obtained; 1) an ECG-triggered prospective calcium score, 2) a prospective ECG-triggered coronary CT angiogram, 3) an ECG-triggered prospective delayed single energy CT (SECT) scan at 5 min and 4) an ECG-triggered prospective delayed dual energy CT (DECT) at 7 min.

- 1) Coronary calcium scoring CT imaging was performed prospectively in systole to maximize LV wall thickness to reduce the risk of contamination from LV blood pool imaging, at 120 kVp, reference mA of 170 mA with CareDose 4D (Siemens Healthineers Erlangen, Germany) to auto adjust according to body habitus. Images were reconstructed with 3 mm slice thickness [24]. The systolic phase images were used as pre-contrast myocardial images.
- 2) Prospective ECG-triggered CT coronary angiograms were acquired in systole at 100-120kVp with automated tube current (CARE dose 4D, Siemens Healthineers Erlangen, Germany). Intravenous contrast (Omnipaque 350 GE Healthcare, Princeton, New Jersey, US) delivery was triphasic (100 % contrast, 40 % contrast and 100 % saline) and bolus tracking used [16].
- 3) A 5-minute, post IV contrast, delayed ECG-triggered, prospective SECT scan, was performed at 30 % phase, 120kVp, reference 170mAs, 1.5 mm section thickness reconstructed to 3 mm thick slices [6].
- 4) A dual energy delayed ECG-gated acquisition was performed 7 min post IV-contrast bolus using 185 effective mAs at 100 kV and 157 effective mA at 140 kV with tin (Sn) filter, 64x0.6 mm collimation. Slices were reconstructed at 3 mm [9].
- 5) All images were acquisitions without overlap between prospectively acquired datasets. Effective radiation exposure was calculated using the dose length product and chest conversion factor ($K = 0.014$ mSv/mGycm) [17].

2.4. CT image analysis (Fig. 1)

CT-ECV image analysis was performed by a level III, Board certified cardiac CT reader with > 10 years experience, blinded to other study data, using Aquarius iNtuition software (Version 4.4.7, TeraRecon Inc, SanMateo, CA, USA) and for dual energy CT analysis: Syngo.via (Siemens Healthineers Erlangen, Germany).

Non-contrast, arterial-phase contrast and 5-minute delayed cardiac images were loaded in a multi-view window (Fig. 1). Regions of interest (ROI) ≥ 100 mm² were drawn following optimization of axial slices by performing double oblique manipulation of multi-reformat images to generate an apical 4 chamber long axis I slice; this was then sliced at 90 degrees to create basal, mid and apical short axis slices. ROIs drawn in the systolic phase bolus-contrast enhanced images were propagated into the systolic non-contrast and 5-minute delayed images (Fig. 1) [9,18].

Myocardial ROIs were drawn in basal, mid and distal short axis slices to calculate ECV in 16 segments. In addition, an apical long axis 4 chamber equivalent view was constructed in order to obtain a single ROI of the basal to mid LV inferior septum [6]. Myocardial ROIs were drawn with careful exclusion of the LV cavity or pericardium; blood pool images were drawn in the LV with careful exclusion of papillary muscle or endocardium. Myocardial and blood Hounsfield attenuation values of the non-contrast and delayed images were used to calculate ECV [6].

2.5. Dual energy CT analysis

Overlay attenuation maps were obtained and LV short axis slices reconstructed at the base, mid and distal levels of the LV. ROIs were drawn (≥ 100 mm²) for LV blood pool and in the LV myocardium to derive standard 16 segment model attenuation values for virtual non-contrast and delayed images (Fig. 2). A single LV myocardial ROI was obtained from reconstructing an apical 4 chamber long axis view and sampling the basal to mid inferior septum [9].

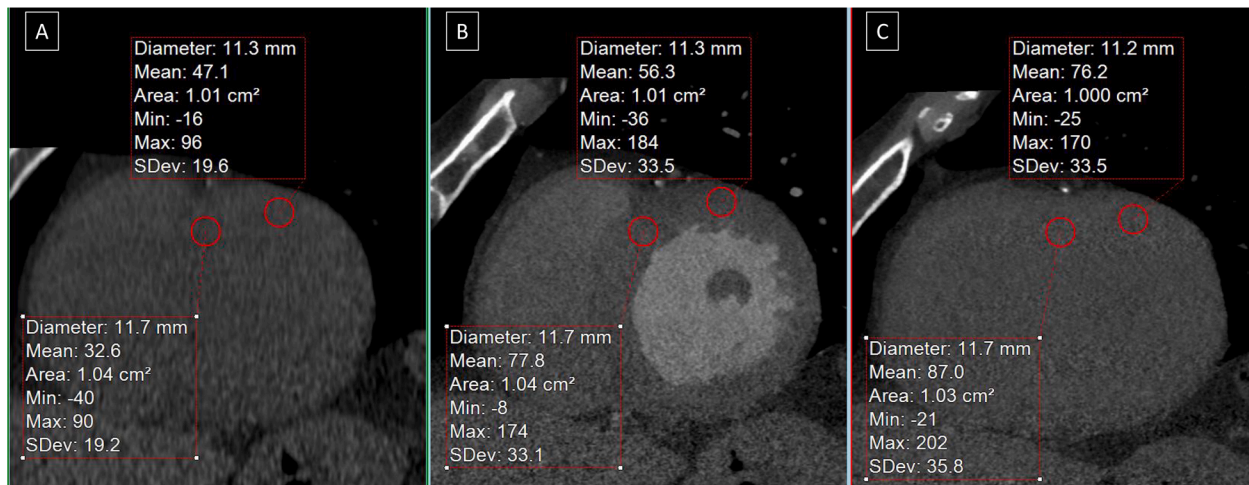


Fig. 1. Assessment of ECV by single energy CT (SECT). Basal short axis left ventricle slices demonstrating sample volumes used in the calculation of ECV. Sample volumes are drawn in the arterial contrast phase image (B) and propagated automatically into the non-contrast (A) image and 5 min delayed image (C). Thus, non-contrast and delayed image sample volume Hounsfield units are derived for the same myocardial volume and ECV can be calculated.

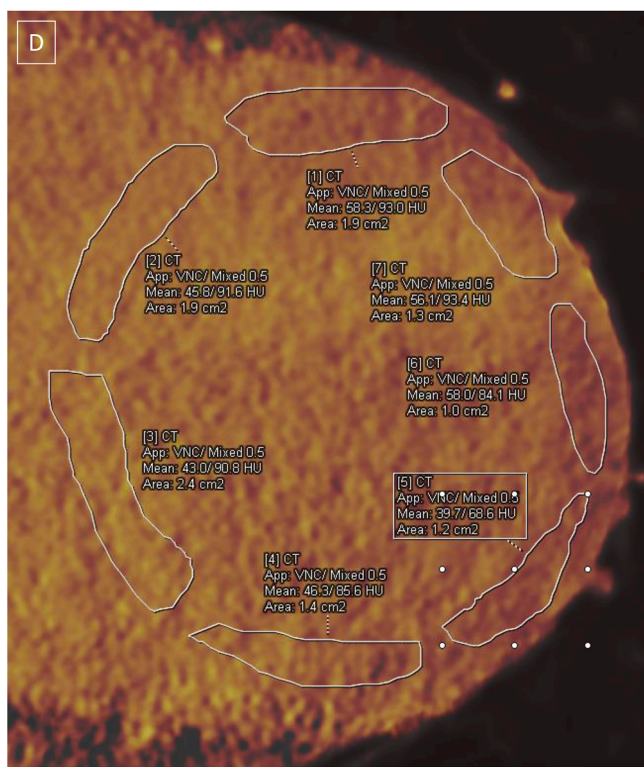


Fig. 2. Assessment of ECV by DECT. An iodine map from DECT acquired data set of a basal left ventricular short axis slice. Sampling volumes are drawn manually. Both virtual non contrast (VNC) and delayed (Mixed) Hounsfield unit are automatically generated for each sample volume.

2.6. ECV analysis by CT

CT ECV was calculated using pre-contrast and delayed images and the following formula:

$$ECV (CT) = (1 - hematocrit) * (\Delta HU_m / \Delta HU_b) * 100 \%$$

ΔHU_m is the change in attenuation of the myocardium in Hounsfield units,

ΔHU_b is the change in attenuation of blood in Hounsfield Units [6].

2.7. Statistics

Comparisons between CT and CMR findings were made on a per protocol basis (SECT or DECT) and on a sampling basis (using single sample volume). A Bland Altman plot was drawn to assess for systematic bias and differences between the techniques. Residuals between CMR and CT values were calculated, and a Pearson correlation coefficient calculated per protocol and per sampling comparisons. The root mean squared errors were also assessed. Comparisons between absolute mean values were performed using the paired *t*-test. To assess technique reliability (a combination of correlation and agreement) intra class correlation coefficients were calculated based on a mean-rating, absolute-agreement, 2-way mixed-effects model with 95 % confidence intervals. Statistical analyses were performed using GraphPad Prism 5 (GraphPad Software, San Diego California US) and IBM SPSS Statistics for Windows, version 28.0 (IBM Corporation, Armonk, New York US). *P* < 0.05 was used as the level of statistical significance.

3. Results

3.1. Patient demographics (Table 1)

From June 2020 to August 2022 25 cardiac amyloid patients were recruited, 24 underwent both single and dual energy cardiac CT. One patient did not complete the dual energy acquisition protocol due to technical issues. The mean age of patients was 80.0 ± 7.1 years, 80 % were male. Of the different types of cardiac amyloid, 4 patients had Light-chain cardiac amyloid AL-CA, 1 had hereditary transthyretin (ATTR)CA and 20 had wild type ATTR-CA (Table 1). Time from CMR to cardiac CT scanning was 2.8 ± 4.0 months.

3.2. Protocol comparisons

Single versus dual energy CT-derived ECV was compared with CMR in 24 patients using paired 16 segment models. 384 paired segments were analyzed. (Fig. 3).

Bland Altman comparisons demonstrated that single energy CT was associated with a small bias toward higher ECV than CMR (0.67 %, 95 % limits of agreement 11.60 to -10.30 %). Root mean squared error values for single energy versus CMR were 5.50 %. Absolute mean error was 5.72 ± 3.77 %. Mean effective radiation dose for single energy CT was 5.49 ± 8.04 mSv.

Dual energy CT was also associated with a small bias to higher ECV in

Table 1
Patient characteristics.

Variable	
Age	80.0 ± 7.12 years
Male	80 %
Hypertension	52 %
Atrial fibrillation	36 %
Amyloid type	
ATTR wild type	80 %
ATTR hereditary	4 %
AL	16 %
NT pro BNP	2909.3 ± 4905 ng/L
Troponin T	56.5 ± 32.3 ng/L
LVEF	48.7 ± 9.7 %
Regional wall thickness	0.68 ± 0.23
CMR Indexed LV mass	144 ± 48.1Kg/m ²
Native T1	1138.5 ± 87.3 ms
Estimated GFR	56.1 ± 19.7 ml/min
Hematocrit	40.5 ± 4.4 %
Delayed single energy CT effective dose	5.49 ± 8.04 mSv
Dual energy CT effective dose	6.90 ± 3.10 mSv

ATTR = Transthyretin amyloid, AL = Light chain amyloid, LVEF left ventricular ejection fraction on echocardiogram, Glomerular filtration rate GFR, N-terminal Brain Natriuretic Peptide (NT pro BNP), cardiac magnetic resonance imaging (CMR).

comparison to CMR (1.80 %, 95 % limits of agreement 7.0 % to -10.60 %) (Fig. 3). Root mean squared error values from dual energy CT versus CMR were 4.75 % and absolute mean error was similar to that observed using single energy CT 6.27 ± 4.70 % (p = 0.619 for comparison to single energy). Correlations were close with both single versus dual energy CT versus CMR (r = 0.79 and 0.88 respectively, p < 0.001 for both) (Figure 5). Mean effective radiation dose for dual energy CT was 6.90 ± 3.01 mSv.

3.3. Intra-class correlation coefficient (ICC)

Reliability of both single and dual energy CT to assess ECV in comparison to CMR was good: ICC for single energy CT was 0.88 (95 % CI

0.73–0.95) and for dual energy was 0.93 (95 % CI 0.82–0.97). Although numerically the average ICC was greater for dual energy CT the confidence intervals of this technique overlapped with single energy CT ICC suggesting a similar reliability of both techniques.

3.4. Sampling comparisons

Single sample volumes from the interventricular septum obtained by SECT or DECT were compared with CMR-ECV values. Bland Altman comparisons demonstrated that SECT was associated with a small bias toward lower ECV than CMR (-2.1 %, 95 % limits of agreement 13.0 to -17.3 %) (Fig. 4). Root mean squared error values for single energy versus CMR were 7.89 %. Absolute mean error was 6.66 ± 4.4 %.

DECT was associated with a small bias to higher ECV in comparison to CMR (1.2 %, 95 % limits of agreement 12.5 to -14.9 %) (Fig. 4). Root mean squared error values from dual energy CT versus CMR were 6.93 % and absolute mean error was similar to that observed using single energy CT 6.94 ± 5.0 % (p = 0.602 for comparison with single energy). Correlations were close with both SECT or DECT versus CMR (r = 0.60 and 0.72 respectively, p < 0.01 for both) (Fig. 4). Absolute mean differences were similar between single and dual energy CT for septal versus global ECV (p = 0.98 and p = 0.80, respectively for single versus dual comparisons).

3.5. Intra-class correlation coefficient (ICC)

There was no difference between the ICC for single energy septal sampling (0.74, 95 %CI 0.42–0.88) versus dual energy (0.84, 95 % CI 0.63–0.93). While average ICC values for both dual and single energy septal sampling could be interpreted as demonstrating good reliability; single sampling techniques were associated with wider confidence intervals suggesting greater variability with single sampling approaches.

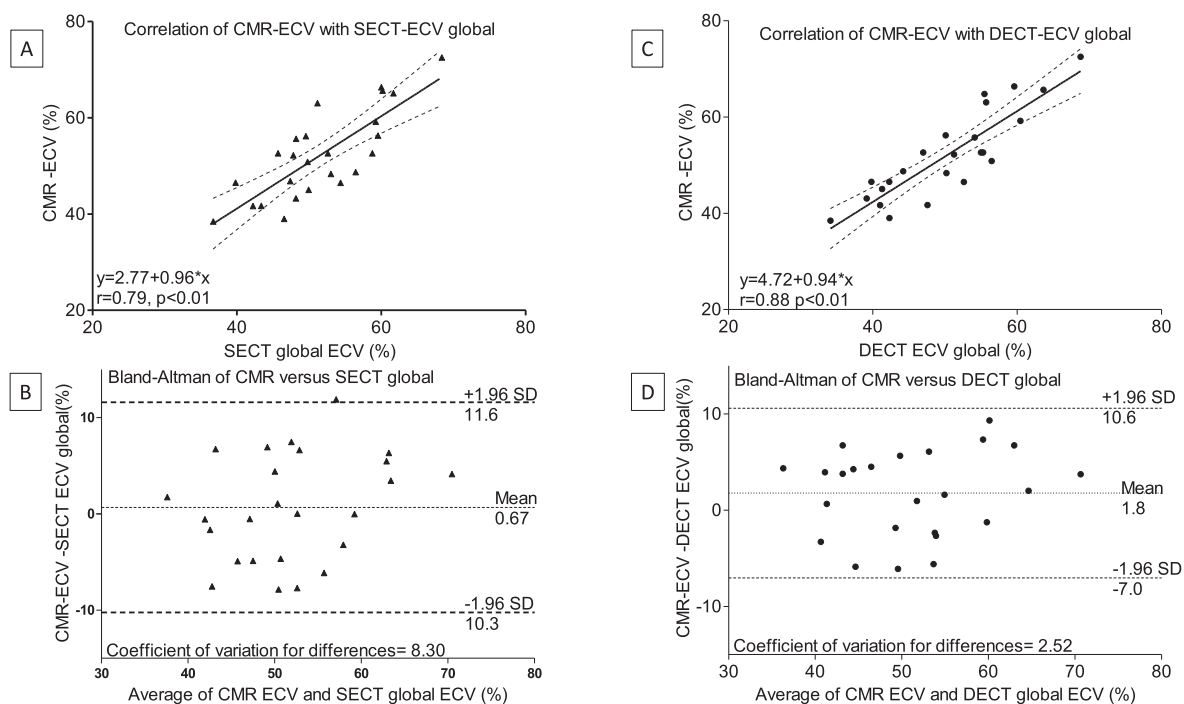


Fig. 3. Protocol comparisons between CMR versus single energy CT (SECT) and dual energy CT (DECT). Correlation and Bland Altman plots for comparisons of CMR-ECV versus global (16 segment) SECT (A and B) or DECT (C and D) derived ECV. Correlation plots dashed lines represent the 95% confidence band.

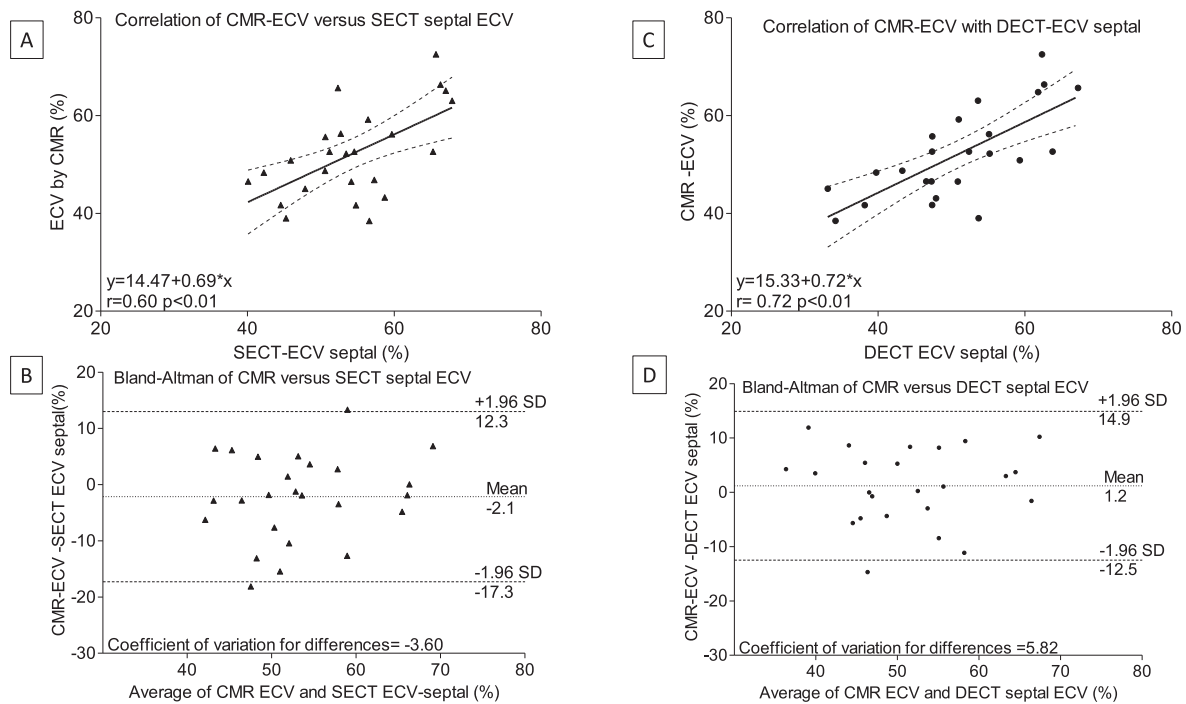


Fig. 4. CMR-ECV versus septal single volume CT-ECV. Correlation and Bland Altman plots for comparisons of CMR-ECV versus single-sample, SECT (A and B) or DECT (C and D) derived ECV. In the correlation plots the dashed lines represent the 95% confidence bands.

4. Discussion

We demonstrated, in a population of cardiac amyloid patients, the correlation of SECT or DECT ECV with CMR-ECV. Both single energy and dual energy CT-ECV were found to have close correlation with CMR. Intraclass correlation coefficients, root mean squared errors and absolute means were comparable between the two CT protocols.

We also considered whether a time-saving single segment CT-derived ECV was comparable with global CMR-ECV. Both SECT or DECT CT single-sample techniques correlated with ECV obtained at CMR. No difference was found between ICCs, root mean square errors and absolute values of septal versus global CT-derived ECV, for either SECT or DECT. Single segment sampling techniques were however associated with greater variability than global derived CT-ECV values and wider confidence intervals on intra class correlation coefficient assessment. Suggesting that more reliable measurement might be obtained using global assessment of ECV versus a septal sampling approach.

With regard to the diagnostic potential of CT-derived ECV, this was not directly addressed in this study. CT derived values did correlate with those found at CMR and, like the values seen at CMR, were elevated to such a high amount as to be highly suggestive of cardiac amyloid. This suggests that CT could be used to assist in the diagnosis of cardiac amyloid. Importantly, only one patient had an ECV by CMR of < 40 % (38 %). On CT, this patient had an ECV of 36 % with dual energy and 37 % using single energy protocols. This was an ATTR wild-type CA patient who presented post TAVI with postural symptoms and a subsequent ^{99m}Tc -pyrophosphate positive study. It is likely therefore that in this case the disease was detected early and this would explain the ECV < 40 % at CMR and CT. The presence of a global ECV of > 35 % is rare in non-ischemic cardiomyopathies other than CA. Thus, considering the present study findings, an ECV \geq 35 % might warrant further testing as a diagnostic threshold.

Others have considered comparisons of DECT versus single energy CT to assess ECV. van Assen et al examined 35 patients with suspected coronary artery disease or cardiomyopathy without cardiac amyloid [11]. In this paper there was no CMR control group. Bland Altman

comparisons between SECT and DECT did not show any systemic bias of one technique over the other. Qi et al compared DECT with CMR 60 normal patients and 60 patients with non-ischemic cardiomyopathy, mean ECV was 31 % [19]. A 16-segment global ECV was derived from CMR and DECT. No systemic bias was noted at Bland Altman comparison and correlation was noted to be close ($r = 0.629$, $p < 0.001$) and similar to that observed in the present study. Wang et al also found close correlation of DECT versus CMR in 35 patients with heart failure, $r = 0.945$, $p < 0.001$ [9].

Single energy delayed imaging was compared with CMR in 26 patients with cardiac amyloidosis by Treibel et al. [6]. Using similar acquisition parameters to the present study, but using single CT sampling volumes, they found close correlation with CMR, $r^2 = 0.85$. This group also demonstrated that a 5-minute time point was preferable to delayed imaging at 15 min in terms of signal to noise ratio. In addition, they demonstrated ECV was greater in ATTR patients versus AL (56 % versus 43 % $p < 0.03$) [6]. In the present study the numbers of AL [4] versus ATTR [21] patients would not permit an accurate comparison between the two types of cardiac amyloid.

Emoto et al compared CMR- ECV with both single and dual energy CT-ECV in 21 patients, 3 of whom were diagnosed with CA [18]. The dual energy technique used to acquire data in this paper was different from the present study. They used a dual-layer spectral detector CT scanner and post processing of non-contrast and delayed images to create iodine density maps. Using a 16-segment model of global ECV, they found close correlations with CMR measure both with iodine map ($r = 0.95$, $p < 0.01$) and single energy protocols ($r = 0.84$, $p < 0.01$). They also showed similar close correlations with CMR-ECV if a single septal segment was used on CT [18].

Using the dual spectral technique to generate iodine maps avoids having to project stenciled sample volumes from arterial phase contrast images to non-contrast and delayed contrast images (Figs. 1 and 2). In the present study similar iodine maps were produced by post processing also avoiding projecting sampling volumes from one myocardial volume to another. Projection of a sample volume from contrast to non-contrast and delayed images can be a potential source of error since projecting

ROIs in this fashion may lead to the inclusion of non-myocardial tissue in projected volumes [3]. It is argued therefore that iodine map reconstructions could theoretically reduce error since iodine map reconstructions calculate virtual non-contrast and post-contrast attenuation values on the same image without the need to project a sample volume between different datasets.

Consistent with this argument, Emoto et al reported a difference in the absolute mean difference of residuals between iodine map and single energy CT techniques and observed higher RMSE for SECT versus iodine map [18]. We did not find any differences in the absolute residuals from DECT using dual source versus SECT in the present study. We do agree though that SECT techniques could be susceptible to error, as described, that can potentially be avoided using DECT imaging.

At present there is no accepted standards for quantifying ECV by CT and no universally agreed protocols [3]. The importance of the current study is to demonstrate that ECV in CA patients can be accurately quantified using both DECT and SECT techniques.

Measurement of ECV by CT might demonstrate utility beyond diagnosis in cardiac amyloid. In AL cardiac amyloid, SECT derived ECV increases with increasing severity of clinical disease and in ATTR cardiac amyloid CT derived ECV predicts prognosis and correlates with bone scintigraphy uptake [13,20]. ECV reduction has also been noted following therapy in ATTR cardiac amyloid- although this was using CMR and similar data from CT is awaited [21].

It is possible that some clinical amyloid centers will adopt cardiac CT as part of a screening assessment of patients with suspected disease or even to track known cardiac amyloid. CT could reduce times to diagnosis and facilitate earlier commencement of therapy in areas where CMR and access to bone scintigraphy/ SPECT are sparse. It is well suited for either role as the CT technology required is widely available and images are rapidly acquired with few absolute contra-indications. Our data add to the growing literature demonstrating close correlation of CT-ECV with that derived from CMR. They also indicate that single segment sampling can be susceptible to wider variation in reliability, perhaps suggesting that a global assessment whether by SECT or DECT techniques would be a preferable approach.

5. Limitations

Ours is a small study of 25 patients, although all patients had cardiac amyloid which is a target population for the technique being tested. Conclusions regarding the diagnostic operating characteristics of cardiac CT for cardiac amyloid cannot be made as the study was not designed to test this. This was a single center study. It would be important for other centers to evaluate the protocols used and compare CT with CMR findings before consideration could be given to adopting either single or dual energy CT techniques into clinical care.

6. Conclusions

Both single and dual energy CT-ECVs were without systemic bias and closely correlated with ECV values obtained by CMR. A single sample derived ECV using CT closely correlated with CMR-ECV but had increased variation in its reliability. Thus, CT measurement of ECV appeared feasible and reliable in cardiac amyloid patients and global assessment may be preferable to avoid variations in reliability.

Declaration of Competing Interest

The authors declare the following financial interests/personal

relationships which may be considered as potential competing interests: [Dr Gary R Small reports a relationship with Pfizer Global Research and Development that includes: funding grants and speaking and lecture fees. Dr Benjamin JW Chow reports a relationship with Siemens Medical Solutions USA Inc that includes: funding grants.].

Appendix A. Supplementary data

Supplementary data to this article can be found online at <https://doi.org/10.1016/j.ijcha.2022.101166>.

References

- [1] P.R. Scully, G. Bastarrika, J.C. Moon, T.A. Treibel, Myocardial Extracellular Volume Quantification by Cardiovascular Magnetic Resonance and Computed Tomography, *Curr. Cardiol. Rep.* 20 (2018) 15.
- [2] N.G. Frangogiannis, The extracellular matrix in myocardial injury, repair, and remodeling, *J. Clin. Invest.* 127 (2017) 1600–1612.
- [3] G.R. Small, A. Poulin, A. Tavoosi, T.D. Small, A.M. Crean, B.J.W. Chow, Cardiac Computed Tomography for Amyloidosis, *Curr. Cardiovasc. Imaging Reports* 14 (2021) 10.
- [4] M. Fontana, R. Chung, P.N. Hawkins, J.C. Moon, Cardiovascular magnetic resonance for amyloidosis, *Heart Fail. Rev.* 20 (2015) 133–144.
- [5] S. Bandula, S.K. White, A.S. Flett, et al., Measurement of myocardial extracellular volume fraction by using equilibrium contrast-enhanced CT: validation against histologic findings, *Radiology* 269 (2013) 396–403.
- [6] T.A. Treibel, S. Bandula, M. Fontana, et al., Extracellular volume quantification by dynamic equilibrium cardiac computed tomography in cardiac amyloidosis, *J. Cardiovasc. Comput. Tomogr.* 9 (2015) 585–592.
- [7] D. Dang, P. Fournier, E. Cariou, et al., Gateway and journey of patients with cardiac amyloidosis, *ESC Heart Fail.* 7 (2020) 2418–2430.
- [8] P.R. Scully, K.P. Patel, B. Saberwal, et al., Identifying Cardiac Amyloid in Aortic Stenosis: ECV Quantification by CT in TAVR Patients, *JACC Cardiovasc. Imaging* (2020).
- [9] R. Wang, X. Liu, U.J. Schoepf, et al., Extracellular volume quantitation using dual-energy CT in patients with heart failure: Comparison with 3T cardiac MR, *Int. J. Cardiol.* 268 (2018) 236–240.
- [10] M. Suzuki, T. Toba, Y. Izawa, et al., Prognostic Impact of Myocardial Extracellular Volume Fraction Assessment Using Dual-Energy Computed Tomography in Patients Treated With Aortic Valve Replacement for Severe Aortic Stenosis, *J. Am. Heart Assoc.* (2021).
- [11] M. van Assen, C.N. De Cecco, P. Sahbaee, et al., Feasibility of extracellular volume quantification using dual-energy CT, *J. Cardiovasc. Comput. Tomogr.* 13 (2019) 81–84.
- [13] F. Gama, S. Rosmini, S. Bandula, et al., Extracellular Volume Fraction by Computed Tomography Predicts Long-Term Prognosis Among Patients With Cardiac Amyloidosis, *JACC Cardiovasc. Imaging* (2022).
- [14] J.D. Gillmore, M.S. Maurer, R.H. Falk, et al., Nonbiopsy Diagnosis of Cardiac Transthyretin Amyloidosis, *Circulation* 133 (2016) 2404–2412.
- [15] C.M. Kramer, J. Barkhausen, C. Bucciarelli-Ducci, S.D. Flamm, R.J. Kim, E. Nagel, Standardized cardiovascular magnetic resonance imaging (CMR) protocols: 2020 update, *J. Cardiovasc. Magn. Reson.* 22 (2020) 17.
- [16] J. Walpot, D. Juneau, S. Massalha, et al., Left Ventricular Mid-Diastolic Wall Thickness: Normal Values for Coronary CT Angiography, *Radiol. Cardiothorac. Imaging* 1 (2019) e190034.
- [17] G.R. Small, M. Kazmi, R.A. deKemp, B.J. Chow, Established and emerging dose reduction methods in cardiac computed tomography, *J. Nucl. Cardiol.* 18 (2011) 570–579.
- [18] T. Emoto, S. Oda, M. Kidoh, et al., Myocardial Extracellular Volume Quantification Using Cardiac Computed Tomography: A Comparison of the Dual-energy Iodine Method and the Standard Subtraction Method, *Acad. Radiol.* 28 (2021).
- [19] R.X. Qi, J. Shao, J.S. Jiang, et al., Myocardial extracellular volume fraction quantitation using cardiac dual-energy CT with late iodine enhancement in patients with heart failure without coronary artery disease: A single-center prospective study, *Eur. J. Radiol.* 140 (2021), 109743.
- [20] P.R. Scully, E. Morris, K.P. Patel, et al., DPD Quantification in Cardiac Amyloidosis: A Novel Imaging Biomarker, *JACC Cardiovasc. Imaging* 13 (2020) 1353–1363.
- [21] M. Fontana, A. Martinez-Naharro, L. Chacko, et al., Reduction in CMR Derived Extracellular Volume With Patisiran Indicates Cardiac Amyloid Regression, *JACC Cardiovasc. Imaging* 14 (2021) 189–199.